STUDY OF THE D.C CONDUCTANCE MECHANISM OF EVAPORATED AMORPHOUS SILICON FILMS

by

YILMAZ ATAĞ

Submitted to the Institute for Graduate Studies in Science and Engineering in Partial Fulfilment of the Requirements of the Degree of

MASTER OF SCIENCE

in

ELECTRICAL ENGINEERING

Boğaziçi Üniversitesi
1984

ACKNOWLEDGEMENTS

I would like to express my sincere gratitute to my thesis supervisors Dr. Yekta ÜLGEN and Dr. Gülen AKTAŞ for their guidance, encouragement and invaluable suggestions during my study.

I would like to thank Doç. Dr. Yani SKARLATOS for the preparation of the films and his valuable suggestions.

ABSTRACT

In this thesis the d.c bulk characteristis of amorphous silicon films are investigated. The films are prepared by electron gun evaporation in a conventional vacuum system. Ohmic contacts are established between the silicon films and the aluminum electrodes. I-V and I-T measurements are performed in the temperaturege range, 110°K to 430° K. Room temperature measurements show that the preparation conditions such as evaporation rate, aging and subsequent annealing all affect the d.c conductivities of the films. In the low temperature range, the data analyzed with the existing models of amorphous semiconductors and the density of states near the Fermi level is calculated. The high temperature data are used to calculate the mobility gap of the amorphous silicon film. The results are then compared with the previously published work.

ÖZETÇE

Bu çalışmada, vakumda buharlaştırma yöntemiyle hazırlanan amorf silikon filmlerin doğru akım gövde karakteristikleri incelenmiştir. Aluminyum elektrodlar ile silikon filmler arasındaki kontağın ohmik olduğu gözlenmiştir. Filmlerin I-V ve I-T ölçümleri 110°K ile 430°K sıcaklık aralığında alınmış olup, oda sıcaklığı dolayındaki ölçümlerde hazırlama koşullarının film doğru akım iletkenliğini nasıl etkilediği araştırılmıştır. Düşük sıcaklıklarda elde edilen veriler var olan amorf silikon modellerinin ışığı altında incelenmiş ve Fermi seviyesi civarındaki durum yoğunluğu hesaplanmıştır. Yüksek sıcaklıklardaki verilerden ise amorf silikon filmlerin iletkenlik bandı hesaplanmıştır. Elde edilen sonuçlar diğer araştırmacıların sonuçları ile karşılaştırılmıştır.

TABLE OF CONTENTS

LIST OF FIGURES

LIST OF TABLES

INTRODUCTION

Since 1960's, amorphous semiconductors have become one of the major research topics of both theoretical and experimental solid state physics. The rapid development in the semiconductor technology during the last two decades with the hope that crystalline semiconductors would be replaced by amorphous semiconductors, which are cheaper to produce, have attracted the interest of many researchers and the number of articles published on this subject has increased at an enormous rate.

The term amorphous is used for materials prepared in the form of a thin film on a cold substrate to prevent crystallization.

The aim of this work is to investigate the d.c characteristics of amorphous silicon films prepared by evaporation, in order to gain a better understanding of the bulk properties.

In the first chapter, a general theory about the structure of amorphous silicon and the temperature dependence of the conductivity is given. The second chapter gives the technique of preparation of the films and the set-up used in the d.c measurements. In the third chapter, the results are given and are analyzed in terms of the effect of preparation conditions on the electrical properties of the films. The results are discussed in comparison with the results of other researchers.

I. THEORY

1.1 STRUCTURE OF AMORPHOUS SOLIDS

In crystalline materials, one first characterizes the ideal periodic structure with a determination of the short-range coordination and through a knowledge of the translational symmetry the long-range order. Further characterization then involves the determination of the concentration of various types of defects and impurities as deviations from the ideal structure.

X-ray diffraction experiments have shown that an amorphous material has a good short-range order; the positions of the nearest neighbours being essentially the same as in the crystalline material.But an amorphous material, unlike a crystal, has no long-range order, so at a distance far from the atom in question the other atoms appear to be randomly distributed. This type of disorder is a positional disorder. In fact, in the amorphous material there is no ideal structure which can be accepted with full confidence.

The previous research on amorphous materials shows that the properties of amorphous films depend strongly on the preparation methods. There are thre basic preparation methods for the amorphous silicon. These are :

1 - Vacuum evaporation

2.- Sputtering

3 - Glow-discharge decomposition of silane (SiH_4)

The specimens prepared by glow-discharge decomposition of silane have fewer

voids and dangling bonds compared to those prepared by evaporation or sputtering techniques (1,2). This is assumed to be caused by the presence of hydrogen during deposition tending to saturate the dangling bonds. The films are structurally heterogeneous when they are deposited on a cold substrate, by evaporation or sputtering. They contain a network of internal voids and dangling bonds, this defect being called the structural disorder.

Because of the extensive disorder present, the Bloch theorem, which is responsible for the extremely high mobilities of free carriers in crystalline semiconductors does not hold for amorphous semiconductors and hence many of the results derived for crystals do not apply directly to amorphous solids. In particular, the concept of the wave vector $\vec{K}$, characterizing the electron wave function, is no longer meaningful. This is also true for the $\vec{K}$-space and Brillouin zones. These concepts, which are direct consequences of the translational periodicity of a crystal lattice, have to be discarded when we consider an amorphous solid. Other concepts used in connection with crystals remain useful however, even in disordered states.

In crystalline semiconductors, the impurity atoms form the impurity energy bands in the forbidden energy gap. These impurity energy bands are narrow and continuous. They constitute localized energy states, like donor and acceptor energy levels closer to conduction band and valence band respectively. In the amorphous semiconductors, however the lack of long-range order and structural defects cause a continuous distribution of localized states in the energy gap.

Davis and Mott (1970) and Cohen, Fritzche and Ovshinsky (CFO) (1969) suggested models for the distribution of the density of localized states in order to explain the conduction mechanisms in amorphous semiconductors (3,4). These two models are illustrated in Figure 1.1 where the shaded regions represent the localized states. In contrast to the crystal, the density of

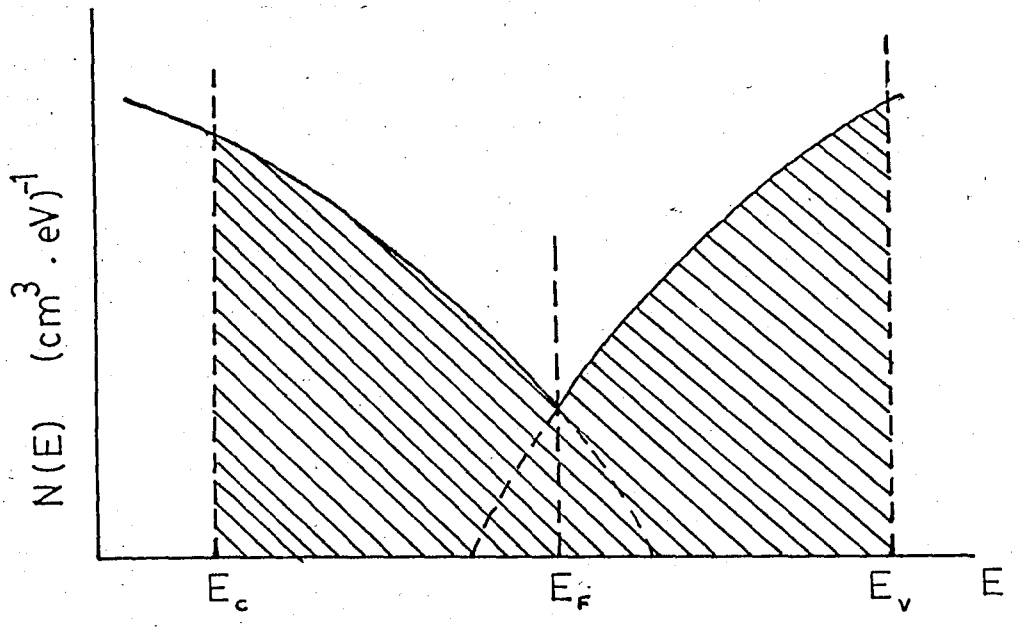

(a)

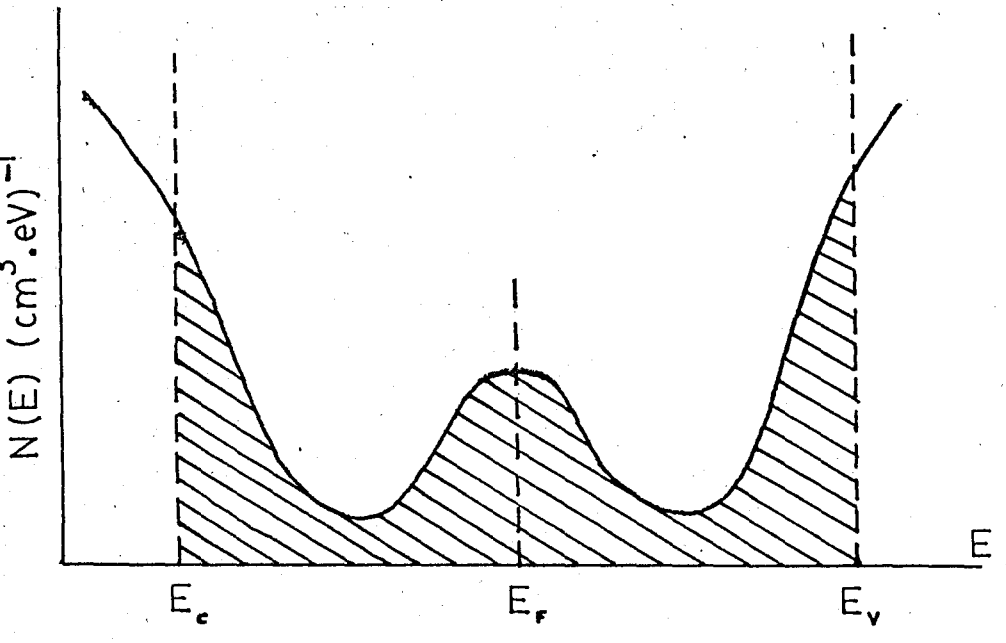

(b)

FIGURE 1.1

Models for the Distribution of the Density of Localized States

(a) Cohen, Fritzche, Ovshinsky Model

(b) Davis and Mott Model

states does not vanish anywhere in the entire range of the energy gap. The density of states extends into the gap from both the conduction band (CB) and valence band (VB). The localized electron states near the band edges are due to the loss of long-range order. The localized states near the middle of the gap originate from the dangling bonds.

In the CFO model, tails of localized states extend from the valence and conduction bands far into the energy gap. Near the center of the gap, these states overlap. When such an overlap takes place repopulation occurs, with electrons transferring from the higher region of the valence band tail into the lower region of the conduction band tail. Since the states are localized, this results in the creation of large concentrations of positively and negatively charged centers or traps. These charged states (donor like and acceptor like states) effectively pin the Fermi level.

In the Davis and Mott model, the tails of localized states do not overlap. The position of the Fermi level is determined by the band of the localized states near the middle of the gap which reaches a maximum at the center and then decreases on both sides.

A common feature of these density of state models is that there is a finite density of localized states at the Fermi energy.

Due to the different character of the electron states, above and below conduction band edge (E_c) and valence band edge (E_v), different conduction mechanism are to be expected. Whereas in the extended states, charged carriers are assumed to move with an almost normal mobility of about 1 to 10 /V-sec, and the transport in localized states can only occur by phonon assisted tunnelling [5]. This is why at the transiton from the extended to localized states at E_c and E_v, the mobility drops sharply by some orders of magnitude giving rise to mobility edges. As a consequence, a pseudo gap, called the mobility gap, E_c-E_v arises.

1.2 THE D.C CONDUCTIVITY IN AMORPHOUS SEMICONDUCTORS AND ITS TEMPERATURE DEPENDENCE

There are two different mechanisms of conductivity in amorphous semiconductors. In the band-to-band conduction at high temperatures, the electrons are excited to the conduction band and holes to the valence band. At low temperatures the conductivity mechanism is dominated by phonon assisted hopping in the regions of localized states.

With the models described for the density of states in the previous section and the mobility edges in an amorphous semiconductor, one would expect three mechanisms of conduction at appropriate temperature ranges :

1- Transport by carriers excited beyond the mobility edges into non-localized (extended) states at E_c or E_v. The conductivity for electrons is

$$\sigma = \sigma_{min} \exp\left[-\frac{(E_c - E_f)}{KT}\right] \qquad 1.1$$

where σ_{min} is the minimum metallic conductivity given by

$$\sigma_{min} = 0.026 \frac{q^2}{\hbar} = \frac{610}{a} \quad (\Omega\text{-cm})^{-1}$$

where a is the interatomic spacing. E_F and E_C are the Fermi energy and conduction band edge energy respectively [3].

2- Transport by carriers excited into the localized states at the band edges and hopping at energies (E^1). For this process, assuming again conduction by electrons, the conductivity is given as,

$$\sigma = \sigma_1 \exp\left[-\frac{E^1 - E_F + W_1}{kT}\right] \qquad 1.2$$

where E^1 is the energy level in the localized state region near the conduction band edge W_1 is the activation energy for hopping at energy E^1, and σ_1 is the preexponential factor [3].

3- If the density of states at E_F is finite, then there will be a contribution from carriers with energies near E_F, which can hop between localized states. We may write for this contribution

$$\sigma = \sigma_2 \exp\left[-\frac{W_2}{kT}\right] \qquad 1.3$$

where w_2 is the activation energy for hopping near the Fermi energy and σ_2 is the pre-exponential factor [3].

At very low temperatures, such as kT less than the bantwidth of the Fermi energy and for a finite density of states near the Fermi energy, the hopping will not be between nearest neighbours, but variable range hopping will take place. For this mechanism of variable range hopping, the conductivity varies as [3],

$$\sigma = \sigma_o \exp\left[-\left(\frac{T_o}{T}\right)^{\frac{1}{4}} \right] \qquad 1.4$$

where

$$T_o = \frac{18\alpha^3}{KN(E_F)} \qquad 1.5$$

and α as the reciprocal of the attenuation distance of the localized wave function, $N(E_F)$ is the density of localized states at E_F and k is the Boltzmann constant [3].

In the temperature range where this equation is valid, $\ln\sigma$ versus $T^{-\frac{1}{4}}$ graph is linear. From the slope of this graph, one can obtain $N(E_F)$ by using proper value of α.

A general graph of temperature dependence of the d.c conductivity is shown in Figure 1.2.

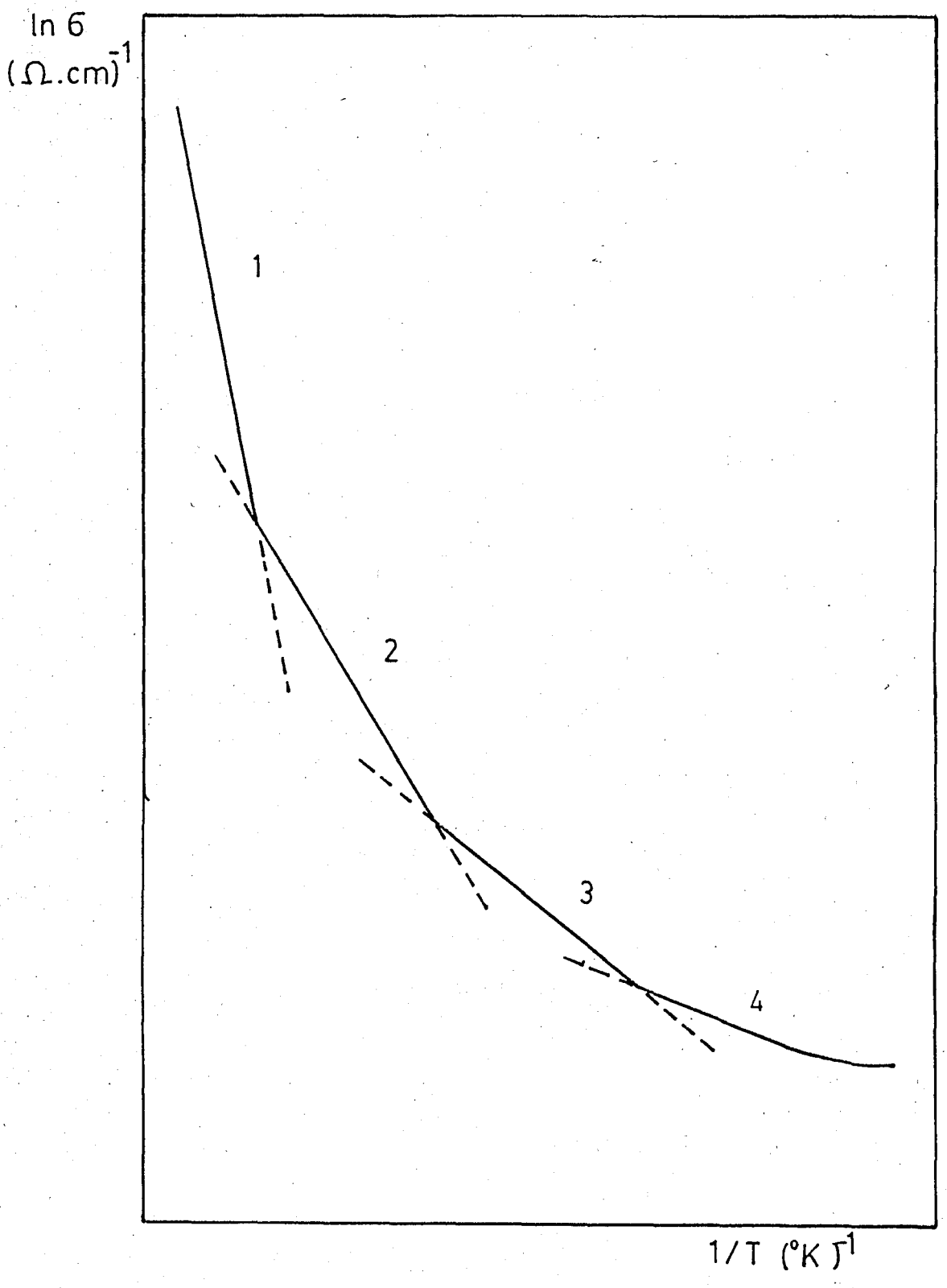

FIGURE 1.2

Temperature Dependence of the d.c Conductivity

Activation Energies : 1- Band to Band Conduction
2- Band Tail Conduction
3- Conduction Due to Hopping to The Nearest Neighbour.
4. Conduction Due to the Variable Range Hopping.

II. EXPERIMENTAL TECHNIQUES

2.1 PREPARATION OF THE FILMS

The amorphous silicon films and metal electrodes are evaporated in a coplanar geometry on microscope slides, by 2.5x4.5 cm in length, produced by Fischer Scientific Co. The masks used in the evaporation process and the metal electrodes are shown in Figure 2.1. The evaporation masks are made of aluminium metal plate of 0.55 mm. thickness. Wires of 0.22 mm, 0.30 mm and 0.37 mm. diameters are placed in the rectangular space (1.5x2.5) of the metal electrode masks to produce a coplanar geometry.

Microscope slides are first cut to the desired dimensions and then cleaned with Alconox detergent in an Ultrasonic vibrator. They are then rinsed with distilled water and methanol.

The vacuum system is VARIAN VT-422 type. The system is pumped down to 10^{-3} torr pressure with a cryopump. In order achieve a lower pressure ion pumps are used. The pumping time of the cryopump is approximately one hour. Ion pumps operate continously for 24 hours to drop the base pressure down to 10^{-7} - 10^{-8} torr. The pressure is measured with a thermocouple-pressure gauge down to 10^{-3} torr and below that value with an ionization-gauge. The glass substrates are placed on a substrate holder, produced by VARIAN, on which three different masks can be placed simultaneously. Therefore three samples can be prepared at a time.

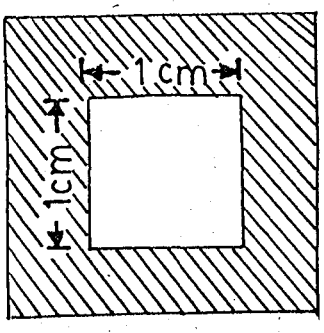

(a)

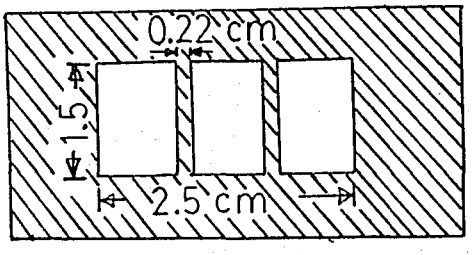

(b)

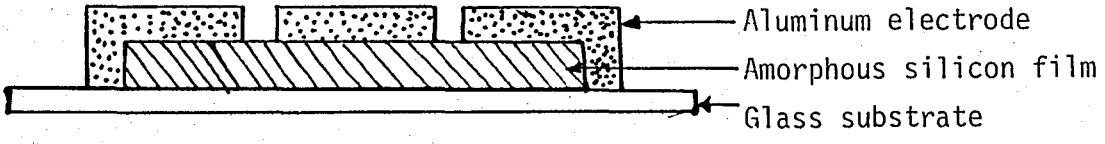

(c)

FIGURE 2.1.

Mask Used in the Preparation of Amorphous Silicon Films

(a) Silicon Mask

(b) Electrode Mask Prepared in Coplanar Geometry

(c) Cross-Section of the Prepared Film in Coplanar Geometry.

The evaporation system used consists of an electron-gun and three crucibles produced by VARIAN. Evaporant is a pure polycrystal hump obtained from Matheson Coleman and Bell laboratories. The distance between the evaporant and glass substrate is 25 cm. The distance must be large in order that most of the atoms reach the substrate along a perpendicular path; otherwise the surface of the film may not be smooth. However, this runs the risk of impurity atom formation on the film. Therefore the base pressure must be kept as low as possible. The base pressure before evaporation could be decreased to 10^{-8} torr and during evaporation it is kept constant at 5-7 10^{-7} torr.

This is achieved by circulating liquid Nitrogen through a jacket around the vacuum chamber. The film thicknessess are between 0.30 μm and 0.60 μm. The evaporation of the silicon films takes between two to four hours. After the deposition of the silicon films, the vacuum system is allowed to cool in order to prevent the formation of an oxide layer on the film. Then the system is opened and prepared for the evaporation of aluminium electrodes. The thickness of the electrodes is around 1 μm. and they are evaporated in 5 to 10 minutes. The thickness of the evaporated films is measured with an A^{o} -scope Interfometer produced by VARIAN. A quartz crystal digital thickness monitor produced by SLOAN is used to adjust the evaporation rate. However, it could not be used to determi the thickness of the films since the density of the films is not known.

2.2 EXPERIMENTAL SET-UP

2.2.1 Thermostatic Room.

During the d.c measurements the samples are kept in a thermostatic room. The schematic diagram of the thermostatic room is shown in Figure 2.2.

By filling the reservoir below the sample holder in the thermostatic room, with liquid Nitrogen, the temperature of the holder can be lowered to-190^{o}

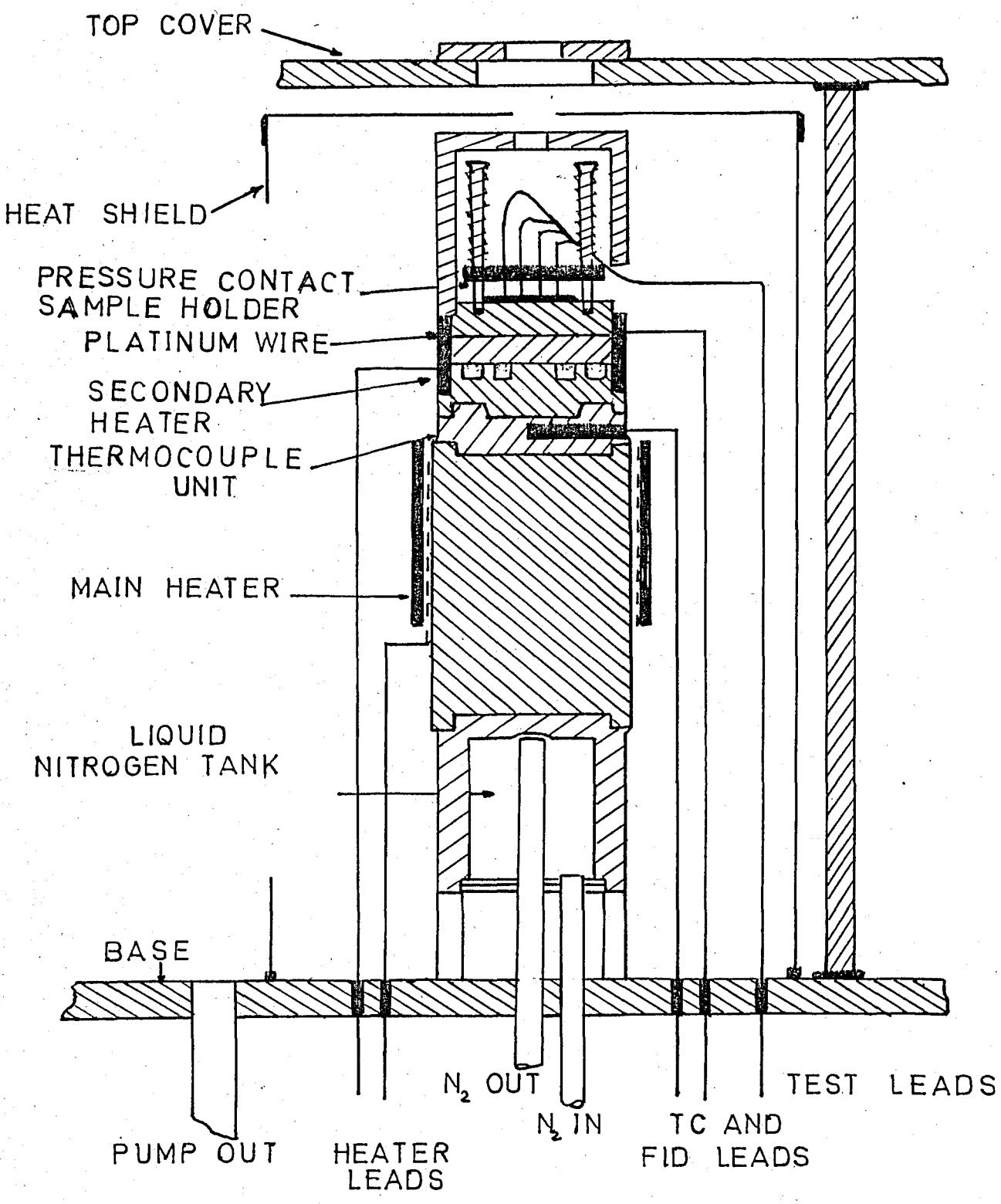

FIGURE 2.2

Schematic Diagram of the Environmental Chamber.

and with aid of two heaters can be raised up to 600°C. By the use of electronic control unit in the thermostatic room, the temperature can be kept constant within ∓ 0.50°C deviations [6]. At lower temperatures, to avoid the condensation of vapor of water and at high temperatures to avoid the oxidization and heat transfer between the thermostatic room and its environment, the air inside the thermostatic room is constantly pumped out.

2.2.2. D.C Measurements.

D.C Measurements include the I-V measurements at room temperature and the I-T measurements at constant electric field. The block diagram of the apparatus used in these measurements is given in Figure 2.3.

According to the applied electric field, the applied voltage is changed manually in 2 volts steps at low electric fields (10^2 V/cm) and in 5 volts steps at high electric fields(10^3 V/cm). The current for each setting is recorded after it became stable to avoid any capacitive effect. Applied voltage is measured with a digital voltmeter connected across the d.c power supply. In fact the digital voltmeter has an internal impedance much lower (1 M Ω) than the resistance of the samples (10^5-10^7Ω) and if the voltmeter were connected across the sample the electrometer would indicate the current through the digital voltmeter and not the sample.

The major difficulty encountered with the high resistivity samples is the environmental noise. For this reason, every connection has to be of shielded type.

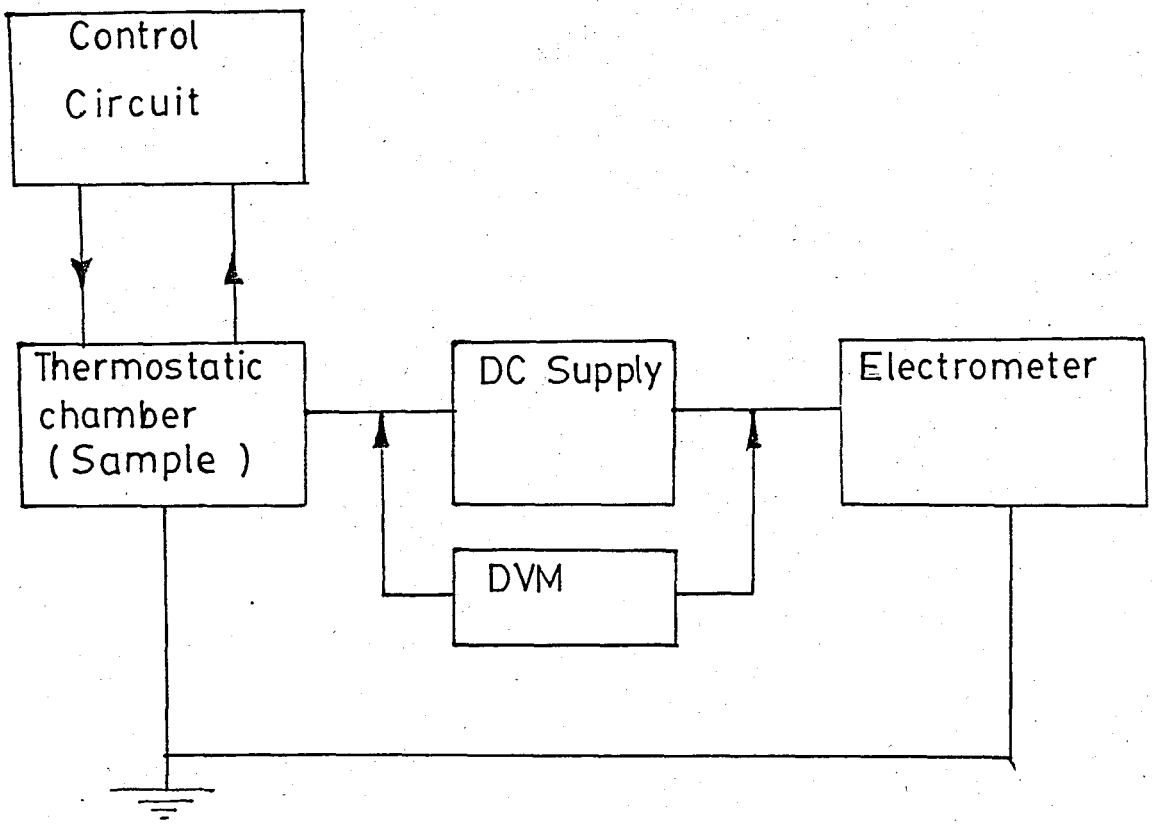

FIGURE 2.3

The Block Diagram of the Apparatus Used in D.C Measurements.

III. EXPERIMENTAL RESULTS

3.1 D.C MEASUREMENTS

The I-V characteristic of the films are obtained using the set-up shown in Figure 2.3, by applying d.c voltage (2V to 75 V) to the samples at room temperature. I-T characteristics of the films are obtained under 10^2-10^3 v/cm. electric fields. Philips PE 1520 is used as the d.c power supply. In order to measure the currents around 10^{-8}-10^{-11} Amp. a Cary 401 vibrating Reed Electrometer is used. To measure larger values of current Keithley Digital Voltmeter is used. During the measurements, the pressure of the thermostatic room is kept as low as 10^{-3} torr.

D.C measurements are done for two purposes:

i) I-V measurements at room temperature are performed to verify whether the contact between the metal electrode and the amorphous semiconductor is ohmic or not and also to gain a better understanding of the preparation conditions effects on the structure of the film.

ii) Temperature dependent conductivity measurements are performed to determine the conductivity mechanism, and the localized state density near the Fermi level.

3.1.1 I-V Measurements at Room Temperature.

The I-V measurements of the samples show that the I-V graph is symmetric with respect to the polarity of the voltage applied implying that the aluminium electrodes form an ohmic contact with the amorphous semiconductor film. There is no contact barrier and the conductivity of the surface states is negligible compared to the conductivity of bulk states.

As seen from Figure 3.1 there is an ohmic region, which goes up to 10^3 V/cm in most samples. The ohmic behaviour disappears after this region and the current increases exponentially at higher electric fields. According to the Poole-Frenkel's theory [7], this is due to the presence of high electric field effects the Coulombic potential barrier. Potential barrier can be lowered such that be thermal energy, which is not enough to release the trapped electron in the absence of the field, becomes sufficent to emit the electron in the presence of the electric field E. In this case the free electron with the help of the electric field, will jump to the conduction band where its contribution to the conduction is considerable The current will therefore be of the form;

$$I = A(T)\, E^{a} \exp\left[\frac{e\beta E^{\frac{1}{2}}}{kT} \right] \qquad 3.1$$

where β is the Poole-Frenkel constant, e is the electron charge, a is the exponent of the order of 1 or 2 and A(T) is a function of temperature. Since the dominant field dependence is through the exponential term, the E^a factor has a relatively weak contribution. A(T) and E^a can be taken as constants. Therefore it is possible to write the current equation in the following form :

$$\ln I = \text{Constant} + \frac{e\beta}{kT} E^{\frac{1}{2}}$$

This shows that a graph of lnI versus $E^{\frac{1}{2}}$ ought to give a straight line with a slope equal to eß/kT. Ln I = $f(E^{\frac{1}{2}})$ graphs for three different samples are shown in Figures 3.2, 3.3 and 3.4 respectively. Here at around 10^3 V/cm electric field and up, the current changes linearly with the square root of the electric field ($E^{\frac{1}{2}}$). This type of behaviour at high electric fields shows that Poole-Frenkel type of conduction is dominant in this region.

3.1.2. The Effect of Preparation Conditions.

It is well known that electrical and optical properties of amorphous semiconductors depend on the preparation conditions [2]. The effect of the preparation conditions on the samples prepared is investigated. All the parameters that can be controlled are systematically changed and the results are as follows;

1- Deposition Rate: The resistivity variations of the films deposited at room temperature with respect to deposition rate is investigated. Decreasing the deposition rate from 1.8 A°/sec to around 0.25 A°/sec increases the resistivity of the films by a factor of 10. This is believed to be due to prevention of the voids accuring during deposition.

Other researchers observed that the density of amorphous silicon is 15 % less that the density of the crystal silicon[8]. This is due to the existence of voids with radii around 40 A° in amorphous silicon. When the deposition rate is kept low, the atoms find time to arrange themselves before they are covered by other atoms. Since in an ideal amorphous silicon there should be no voids, consequently no dangling bonds and impurity atoms, the density of localized states around the Fermi level should be low meaning

increasing resistivity. Only then the impurity atoms forming the base pressure have chance to stick to the film. Therefore during the deposition, the base pressure is kept as low as 10^{-7} torr.

2- Ageing : I-V measurements of the same sample are obtained at different times and the change in resistance is observed. In the course of time, as it is seen in Figure 3.5 the resistivity is increased. This effect is observed one month following the film deposition, later on the film is stable.

3- Annealing : The samples are annealed at around 300^{o}C. As a result of annealing, the resistivities of the films deposited at room temperature are increased by a factor of 10.

The effects of preparation conditions on the resistivities of the films are given Table 3.1. With lower evaporation rate, againg and annealing, the highest resistivity which is obtained, is 10^{7} Ω-cm. The resistivities of the amorphous silicon films prepared with the electron gun evaporation method by other researchers are as following [9,10 and 11].

Researchers	Resistivity (Ω-cm)
Yong, John and Wong	10^{7}-10^{8}
Dey and Fong	10^{5}-10^{6}
Delleferra, Labusch and Roscher	10^{3}-10^{4}

3.1.3 Study of The d.c Conductivity as A Function of Temperature

Current versus temperature (I-T) measurements are performed between 110°K and 430°K at constant electric field at 10°C or 20°C temperature intervals. The results obtained for two samples are shown in Figures 3.6 an 3.7.

In the higher temperature range, the conductivity mechanism involved is band-to-band conduction. The temperature at which band-to-band conduction

TABLE 3.1

Sample no.	Evaporation Rate. (Å/Sec)	Evaporation Pressure. (Torr.)	Thickness (Å)	Resistivity Before Annealing ρ (Ω-cm)	Resistivity After Annealing. ρ (Ω-cm)
23.4.84-I	1.8	6×10^{-7}	6000	6×10^{3}	
23.4.84-II	1.8	6×10^{-7}	6000	1.1×10^{4}	1.1×10^{5}
23.4.84-III	1.8	6×10^{-7}	6000	1×10^{4}	
22.5.84-I	0.25	6×10^{-7}	3600	1.6×10^{5}	2.4×10^{5}
22.5.84-II	0.23	6×10^{-7}	3314	1.5×10^{5}	
22.5.84 III	0.27	6×10^{-7}	3883	1.7×10^{5}	
7.7.84-I	0.28	5×10^{-7}	4772	6.1×10^{6}	2.7×10^{7}
7.7.84-II	0.36	5×10^{-7}	6079	8.8×10^{6}	
7.7.84-III	0.26	5×10^{-7}	4422	5.2×10^{5}	

Note: All data are taken at room temperature

occurs must be determined. In order to determine the temperature above which the basic transport mechanism is band-to-band conduction the conductivity versus temperature graphs are constructed. The results for the samples are shown in Figures 3.8, 3.9 and 3.10.

The activation energies obtained from the slope $\ln\sigma$-versus-T^{-1} graphs above 130°C are around 0.8-0.54 eV, which are the half of the energy gap. These values show that the mobility gap of amorphous silicon lies around 1.1-1.6 eV. These values agree with the values obtained by other researchers[13]. Therefore at temparatures above 130°C the conductivity mechanism is a band-to band conduction.

In the high temperature range, between 403°K and 285°K a different conduction mechanism exists since the curve is not linear any more. In this temperature range electrons jump to tail states closer to the conduction band.

At temperatures between 285°K and 200°K, the dominant conductivity mechanism is of the form :

$$\sigma = \sigma_2 \exp\left[- \frac{\Delta E}{kT} \right] \qquad 3.3$$

The activation energies obtained from the slopes of $\ln\sigma$ versus T^{-1} graphs between 285°K and 200 °K are between 0.2 and 0.06 eV.This shows us that the conductivity mechanism involved is not band-to-band conduction but it is rather hopping conduction between the nearest neighbours.

3.1.4 Measurement of the Density of States.

In the low temperature range below 200°K and at constant electric field of 10^2-10^3 V/cm. the conductivity versus $T^{-\frac{1}{4}}$ graphs of the samples are plotted. These graphs are shown in Figures 3.11 and 3.12. In this temperature range there is a linear relation, in accordance with the variable range hopping conductivity proposed by Mott. The equation (1.4)

can be rewritten as,

$$\ln\sigma = \ln\sigma_o - \left(\frac{T_o}{T}\right)^{\frac{1}{4}} \qquad 3.4$$

Therefore the density of localized states around the Fermi level, $N(E_F)$, can be calculated using the slope of the $\ln\sigma$ versus $T^{-\frac{1}{4}}$ graph. By taking $\alpha^{-1} = 10\ \text{A}^{\circ}$ as proposed by Mott [3] for evaporated silicon films, the $N(E_F)$ values are calculated for the samples. The results are as follows :

Sample no	$N(E_F)$ $(cm^3\text{-}eV)^{-1}$
23.4.84 - II	1.46×10^{20}
22.5.84 - I	2.7×10^{21}
2.7.84 - I	2.5×10^{20}

These results are in good agreement with the values obtained by other experimenters [12], and show that the dangling bonds are highly concentrated around the Fermi level.

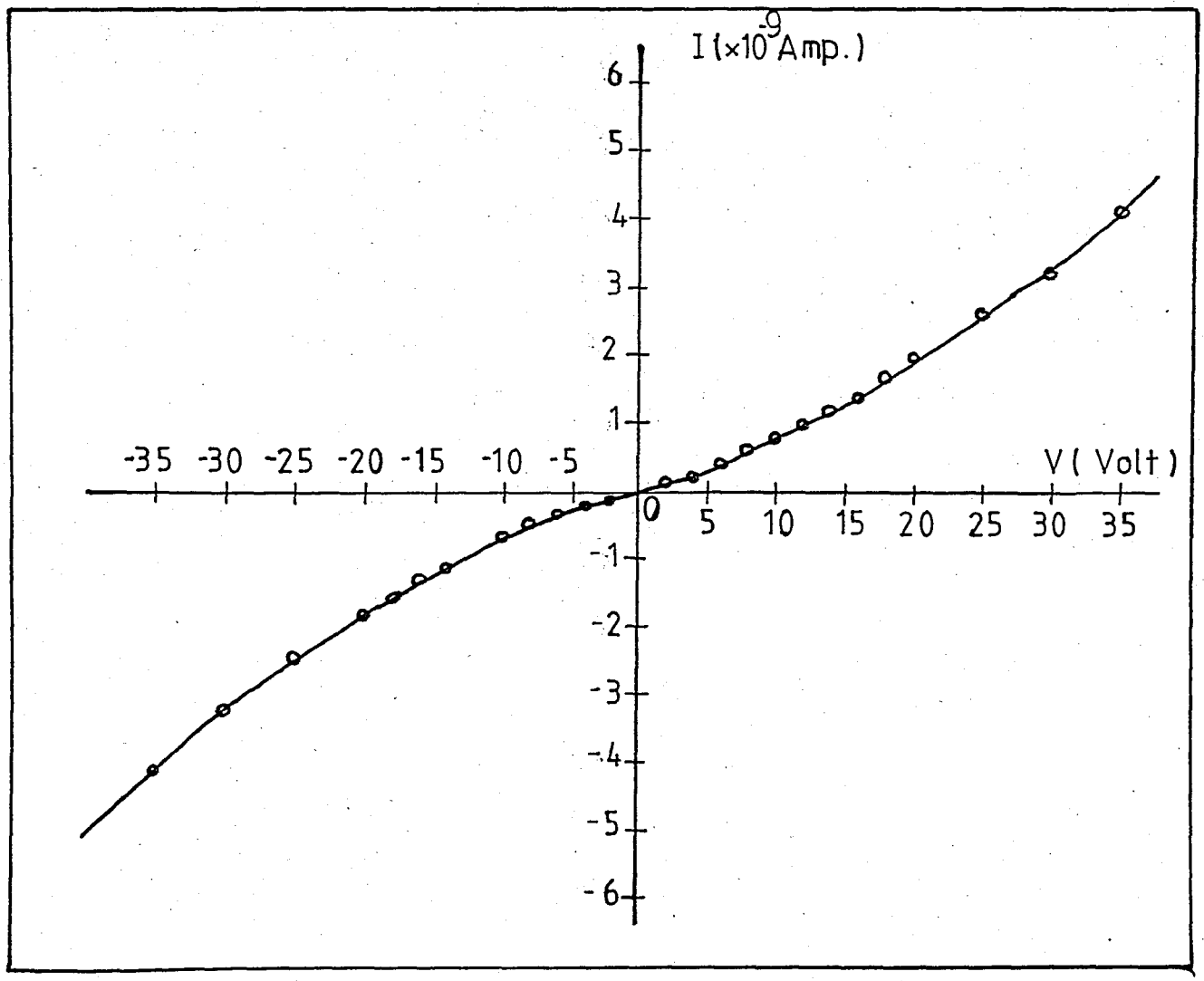

FIGURE 3.1

Typical I-V Curve of a Sample at Room Temperature

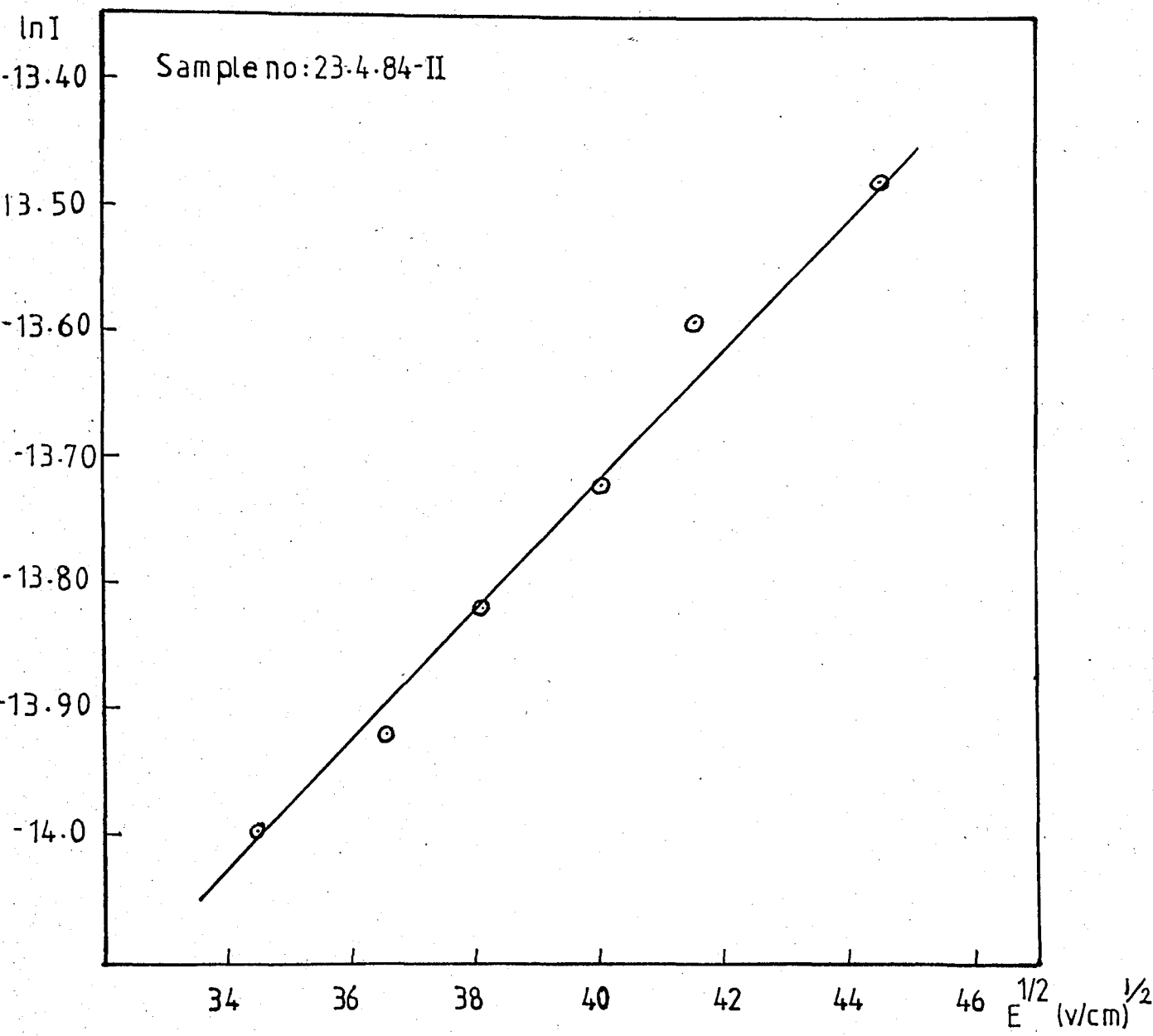

FIGURE 3.2

LnI versus $E^{\frac{1}{2}}$ graph of the sample no:23.4-84-II at Higher Electric Fields Between 1156 V/cm to 2116 V/cm.

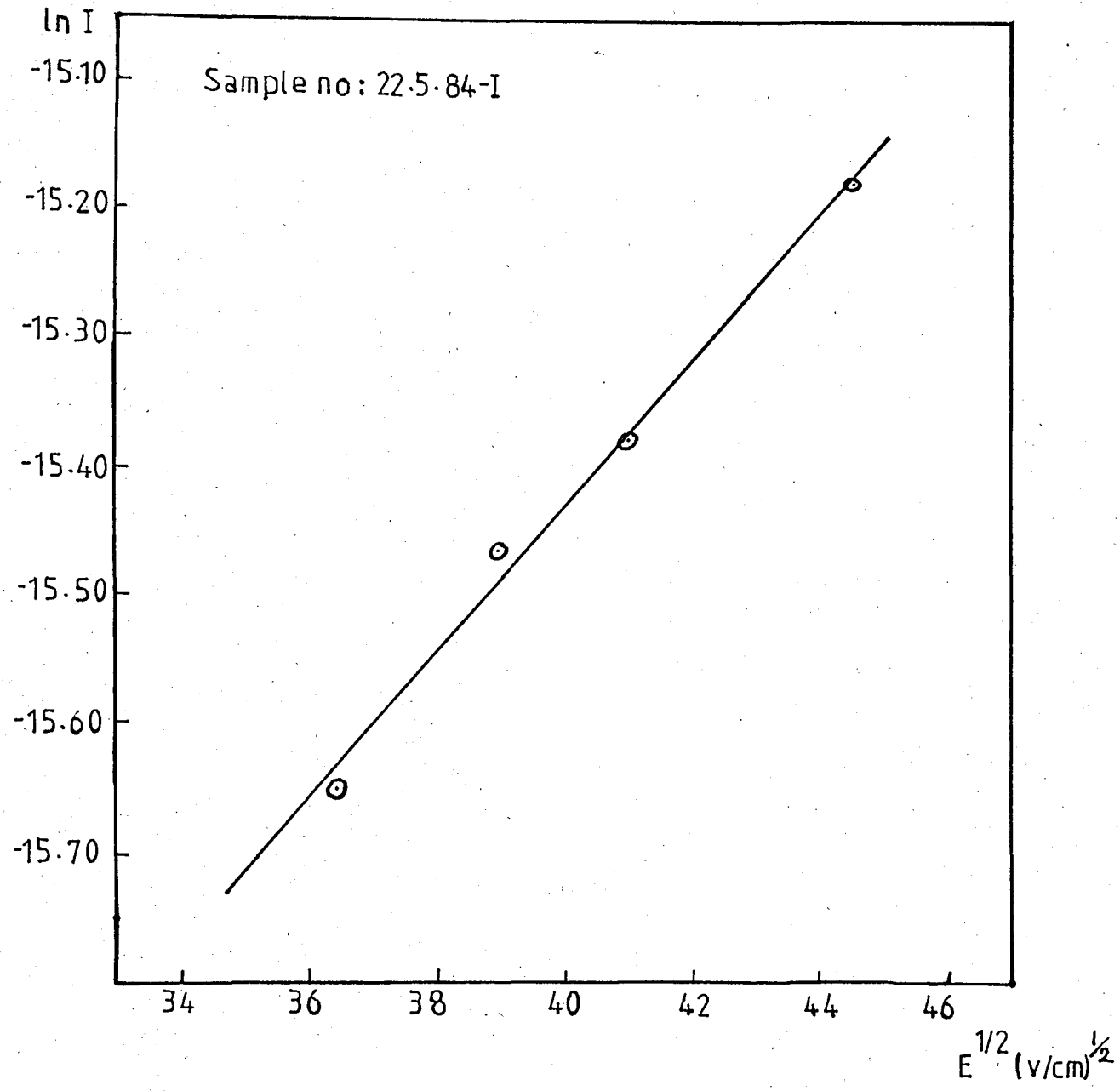

FIGURE 3.3

LnI versus $E^{\frac{1}{2}}$ Graph of the sample no:22.5.84-I at Higher Electric Fields Between 1296 V/cm to 2116 V/cm.

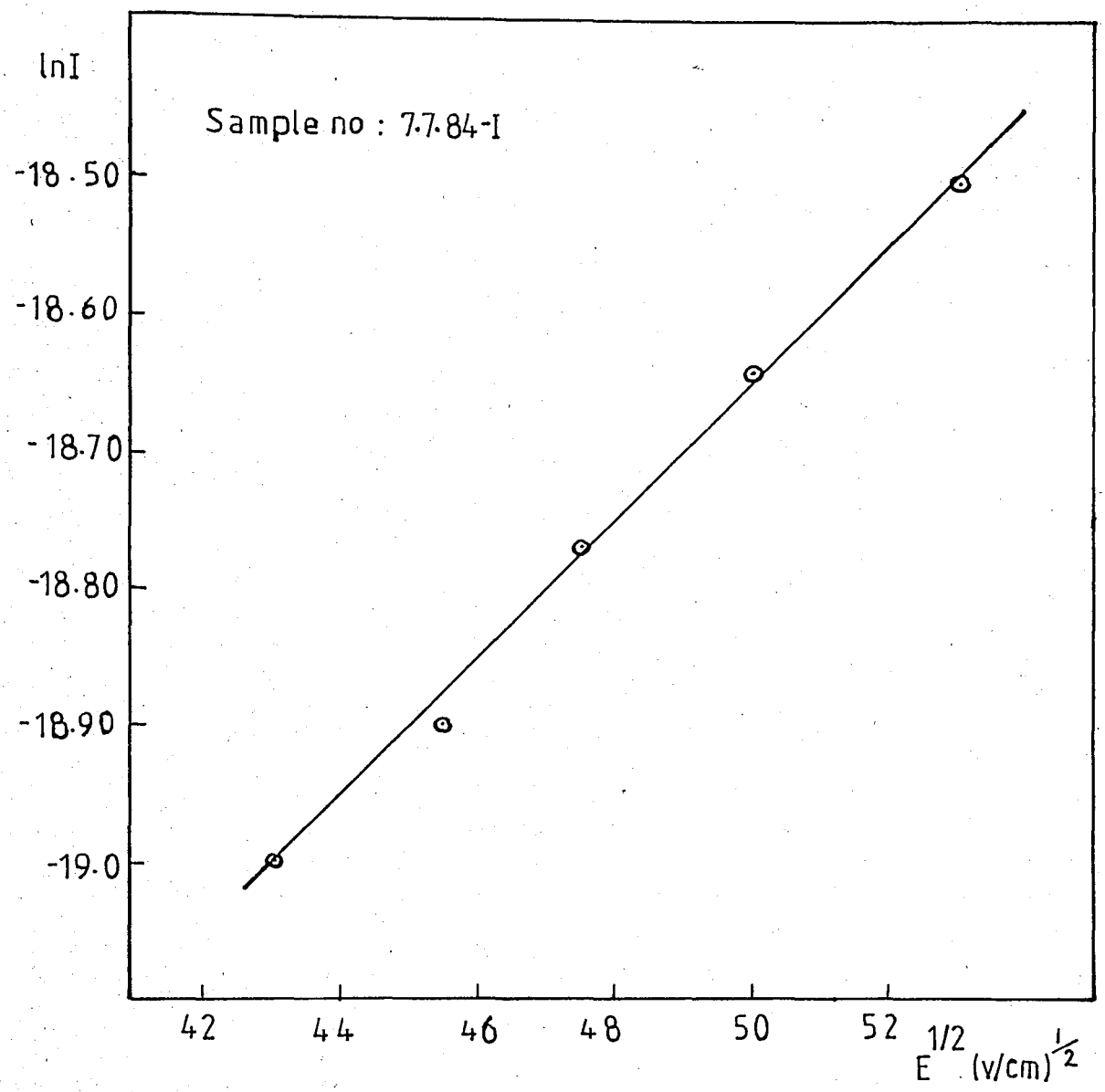

FIGURE 3.4

LnI versus $E^{\frac{1}{2}}$ Graph of the sample no: 7.7.84-I at Higher Electric Fields Between 1849 V/cm to 2809 V/cm.

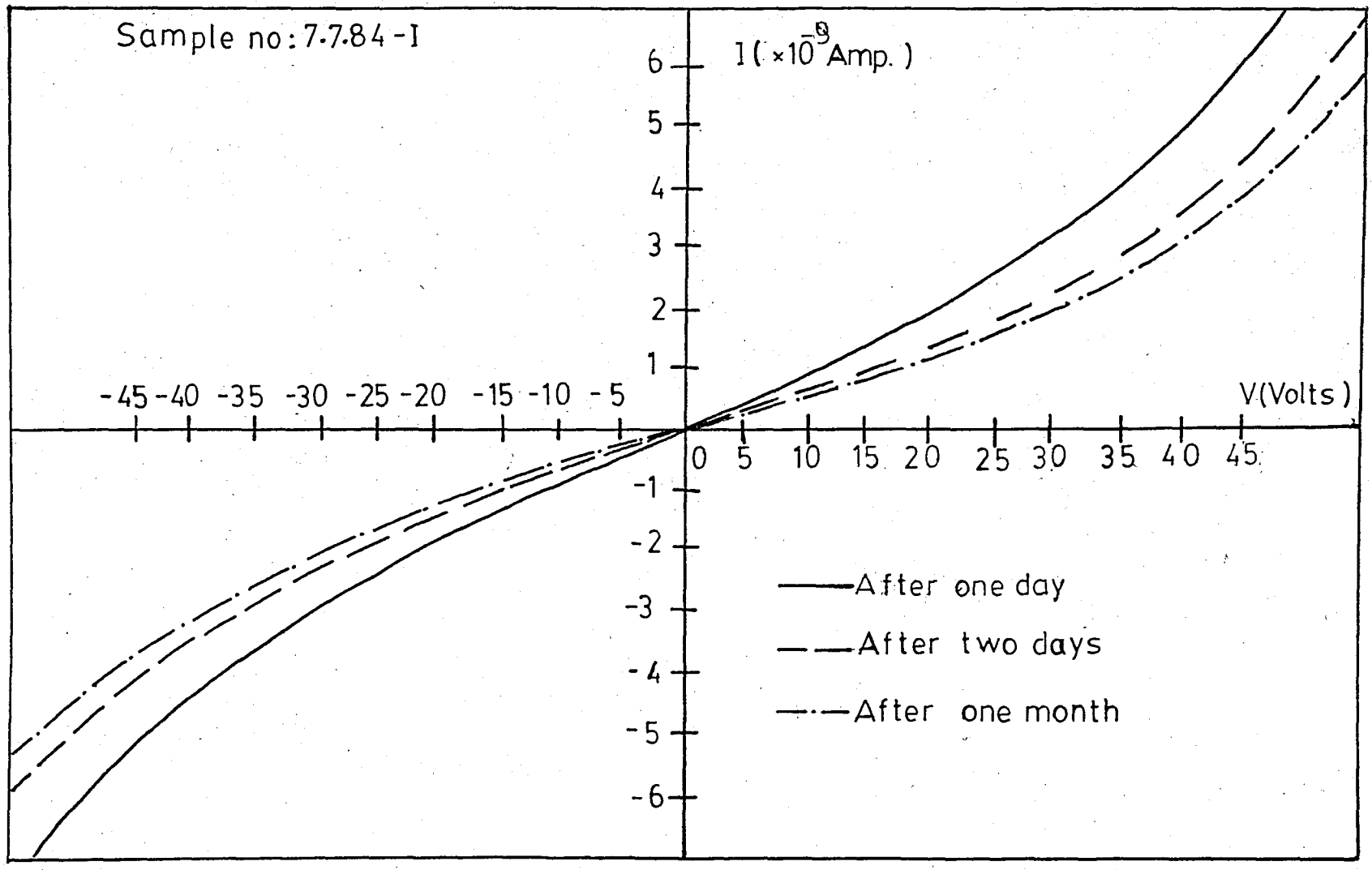

FIGURE 3.5

The Change of Resistivity with Time.

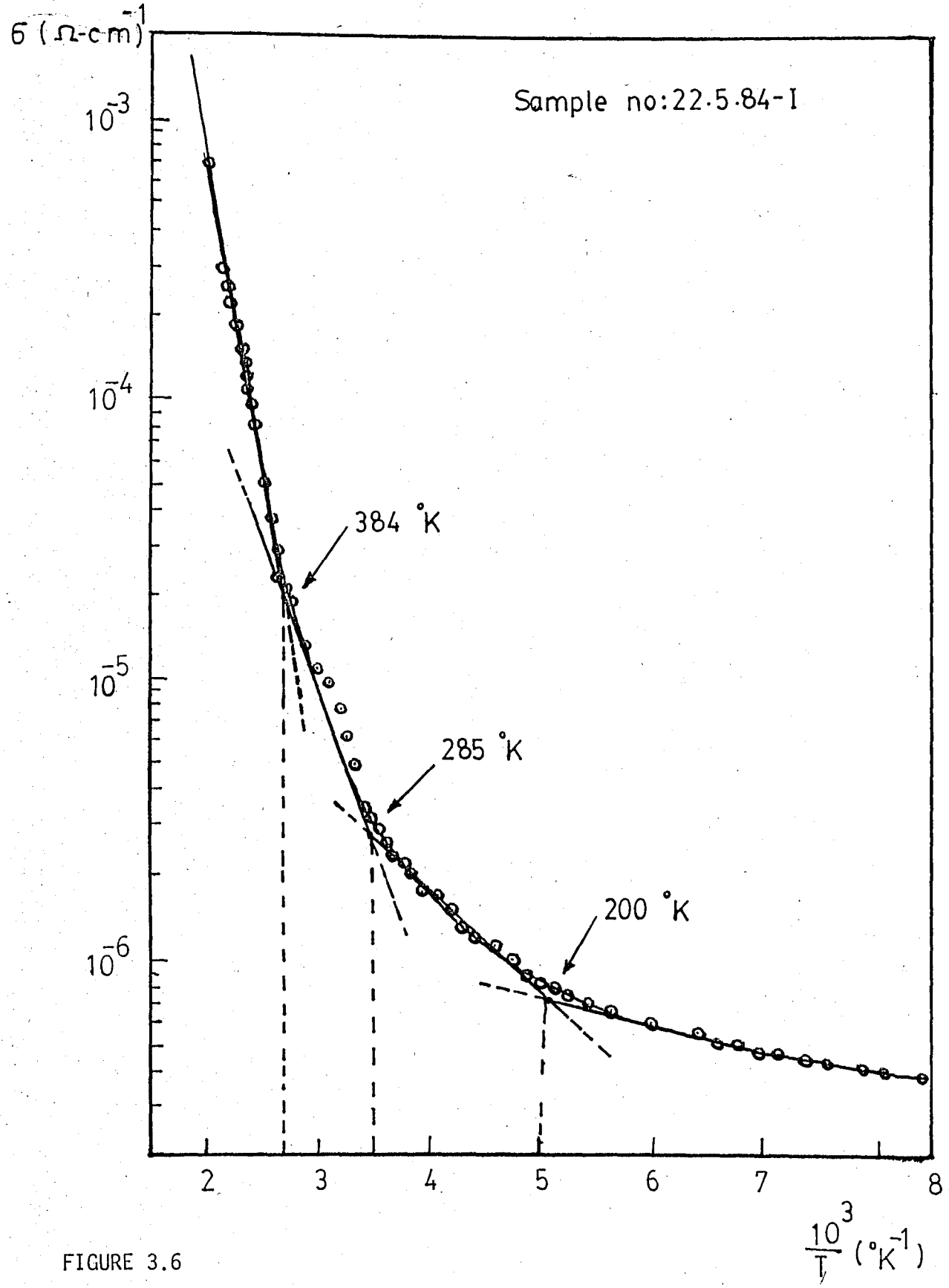

FIGURE 3.6

The Conductivity of The Sample is Plotted for The Full Temperature Range 110°K to 430°K

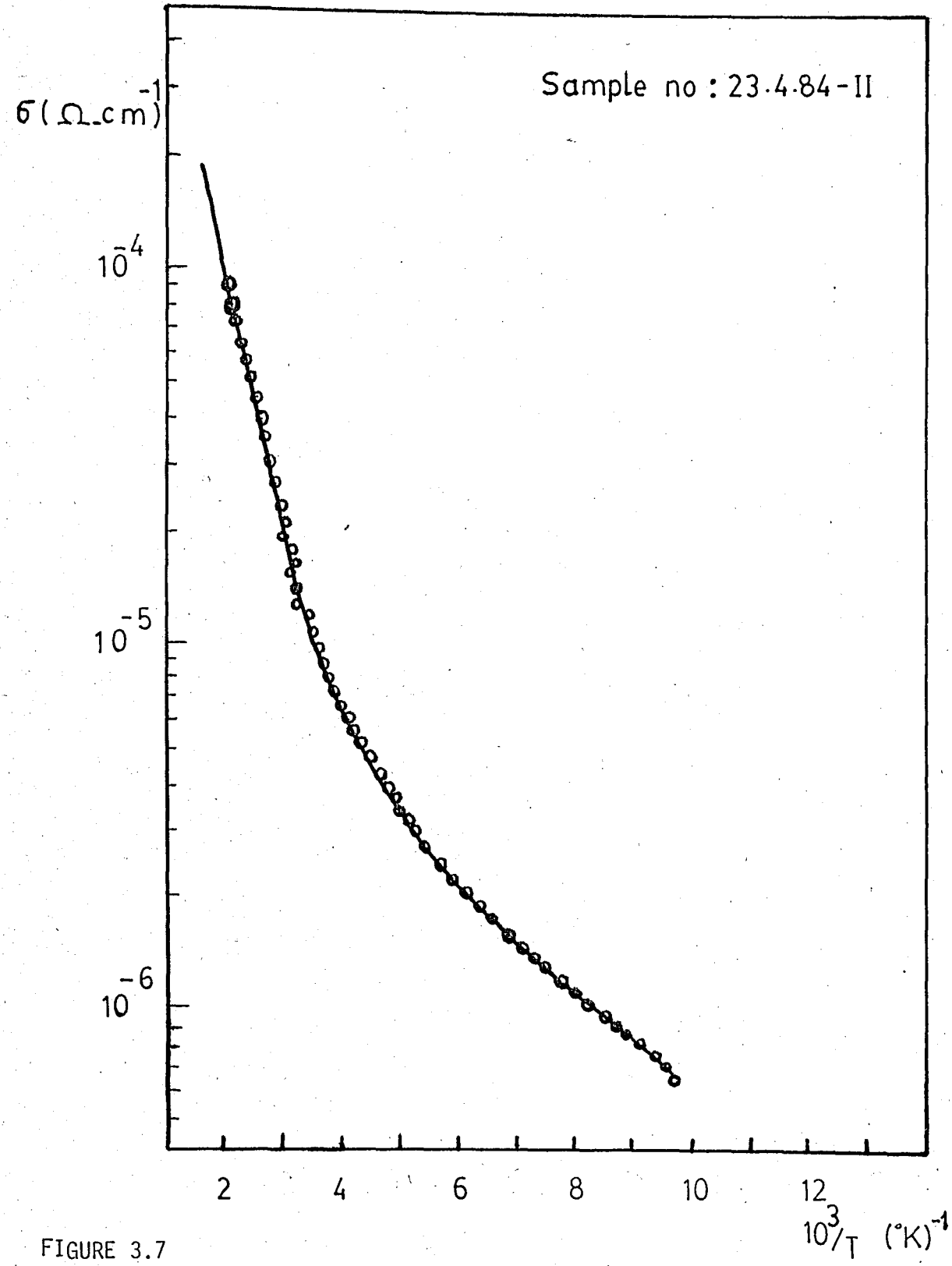

FIGURE 3.7

The Conductivity versus T^{-1} Graph of the Sample no:23.4.84-II for the Full Temperature Range 100°K to 400°K.

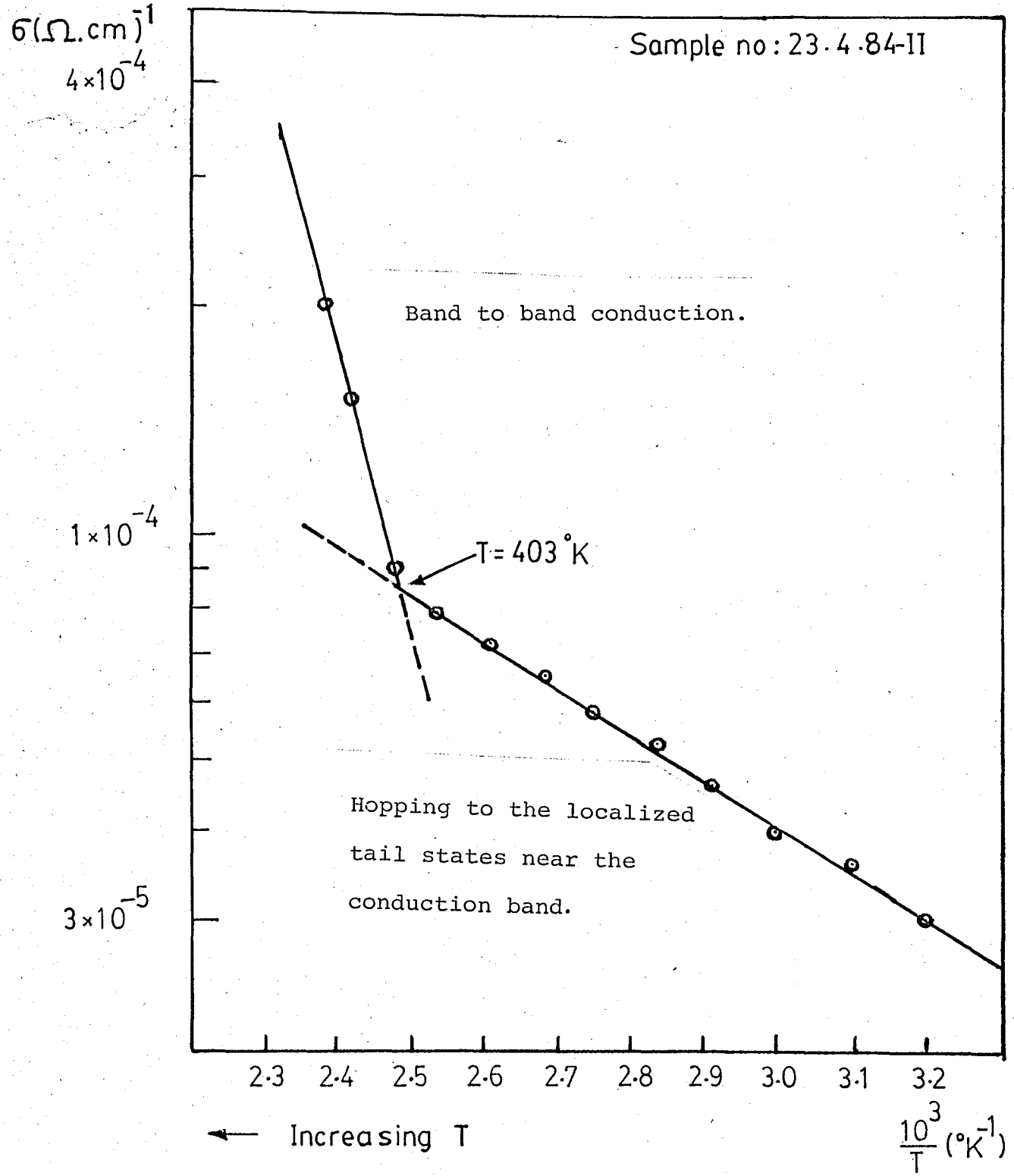

FIGURE 3.8

The Conductivity versus T^{-1} Graph of the Sample no: 23.4.84-II for the Temperature Range 312°K to 435°K.

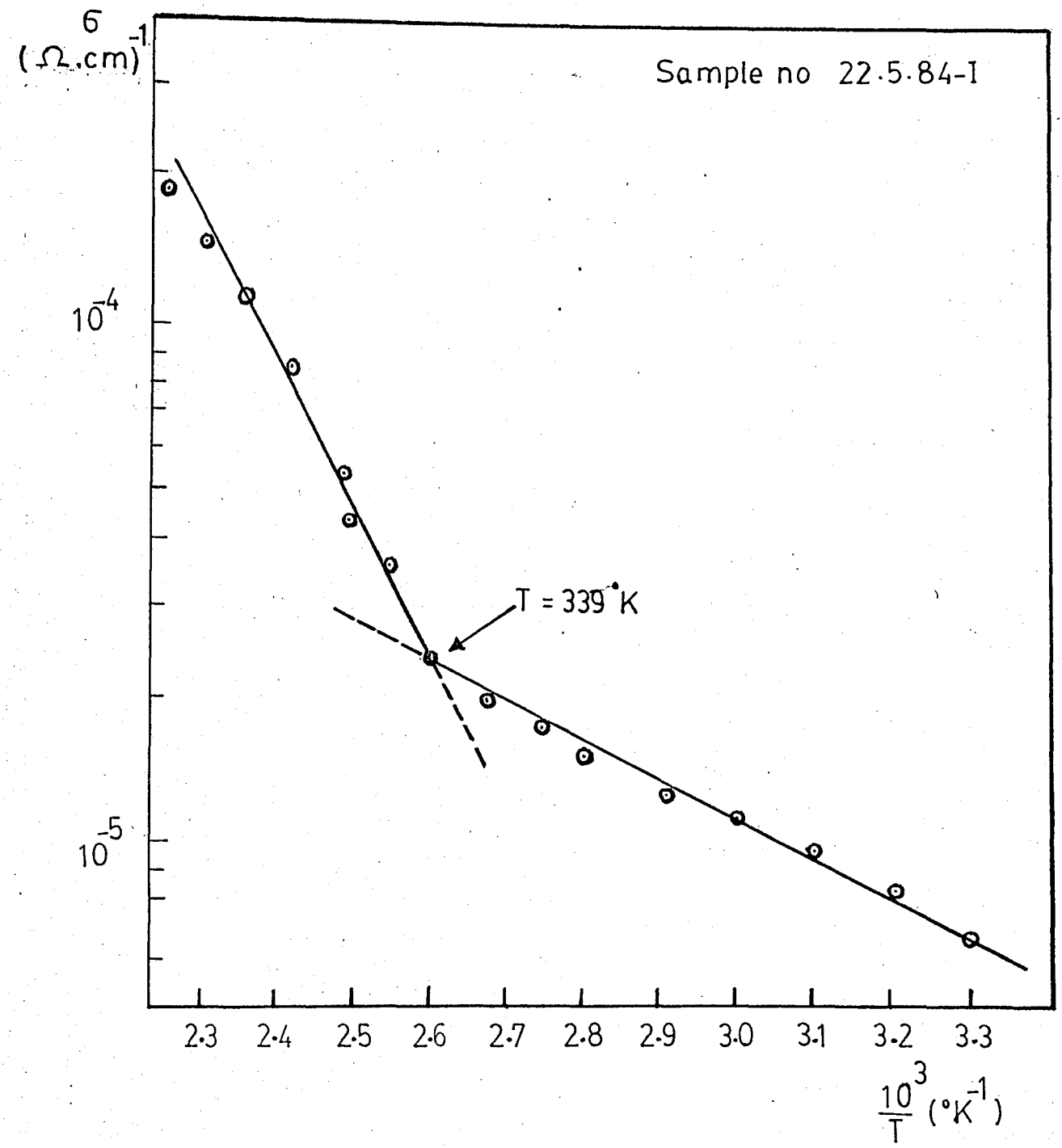

FIGURE 3.9

The Conductivity versus T^{-1} Graph of the Sample no:22.5.84-I for the Temperature Range 303°K to 454°K.

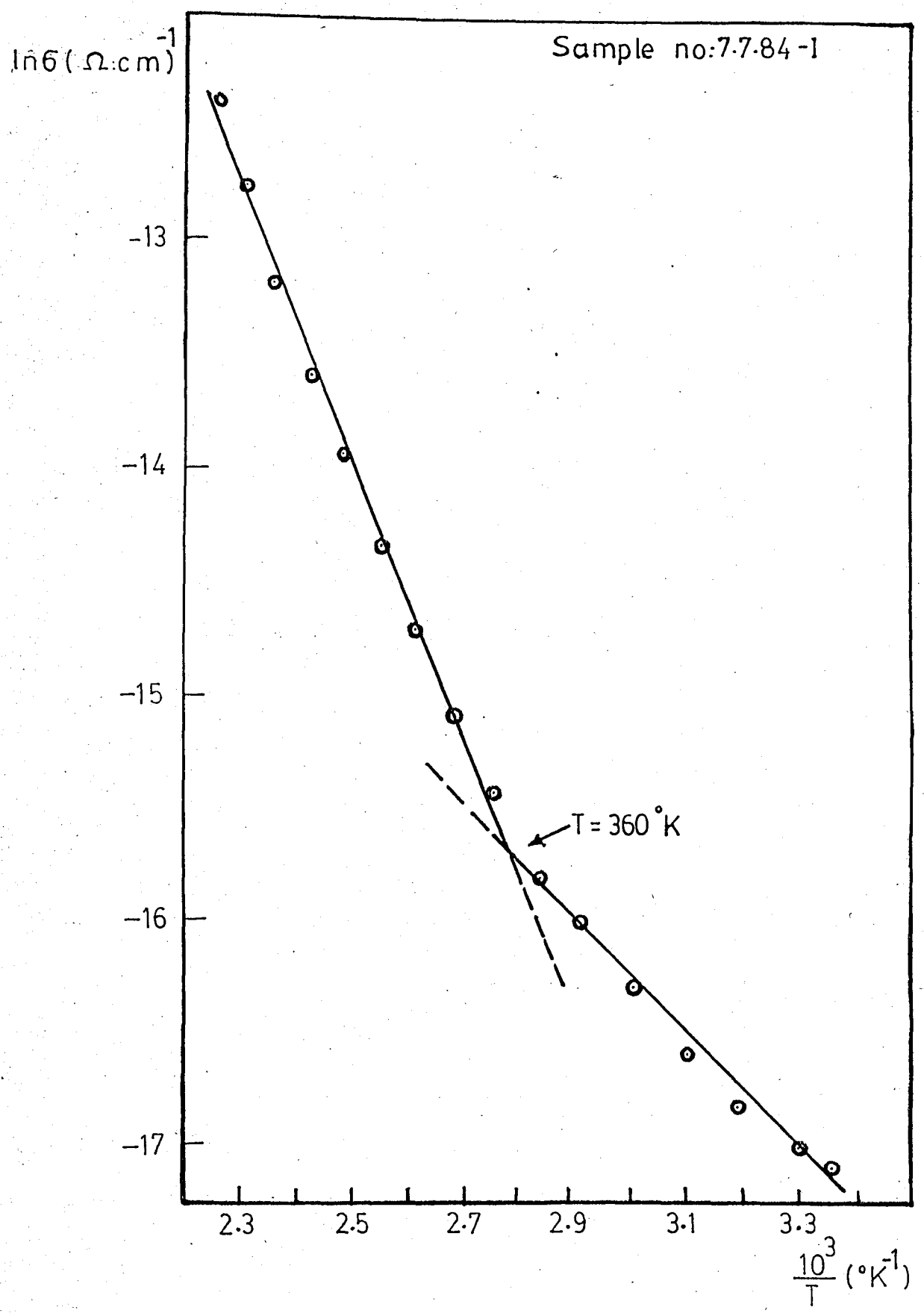

FIGURE 3.10

The Conductivity versus T^{-1} Graph of the Sample no: 7.7.84-1 for the Temperature Range 298°K to 444°K.

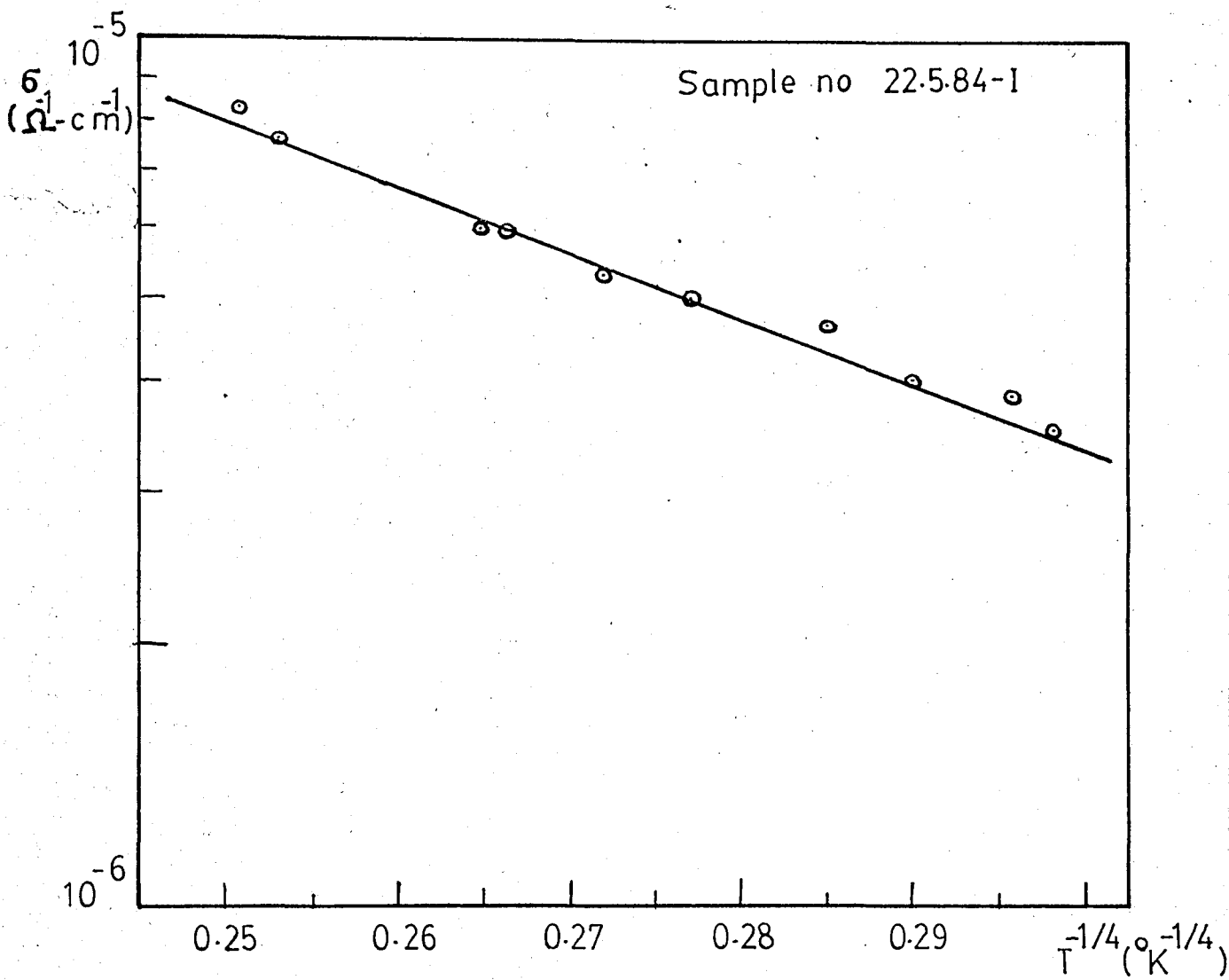

FIGURE 3.11

The variation of conductivity as a function of $T^{-\frac{1}{4}}$ for the low temperature range, between 256°K to 118°K.

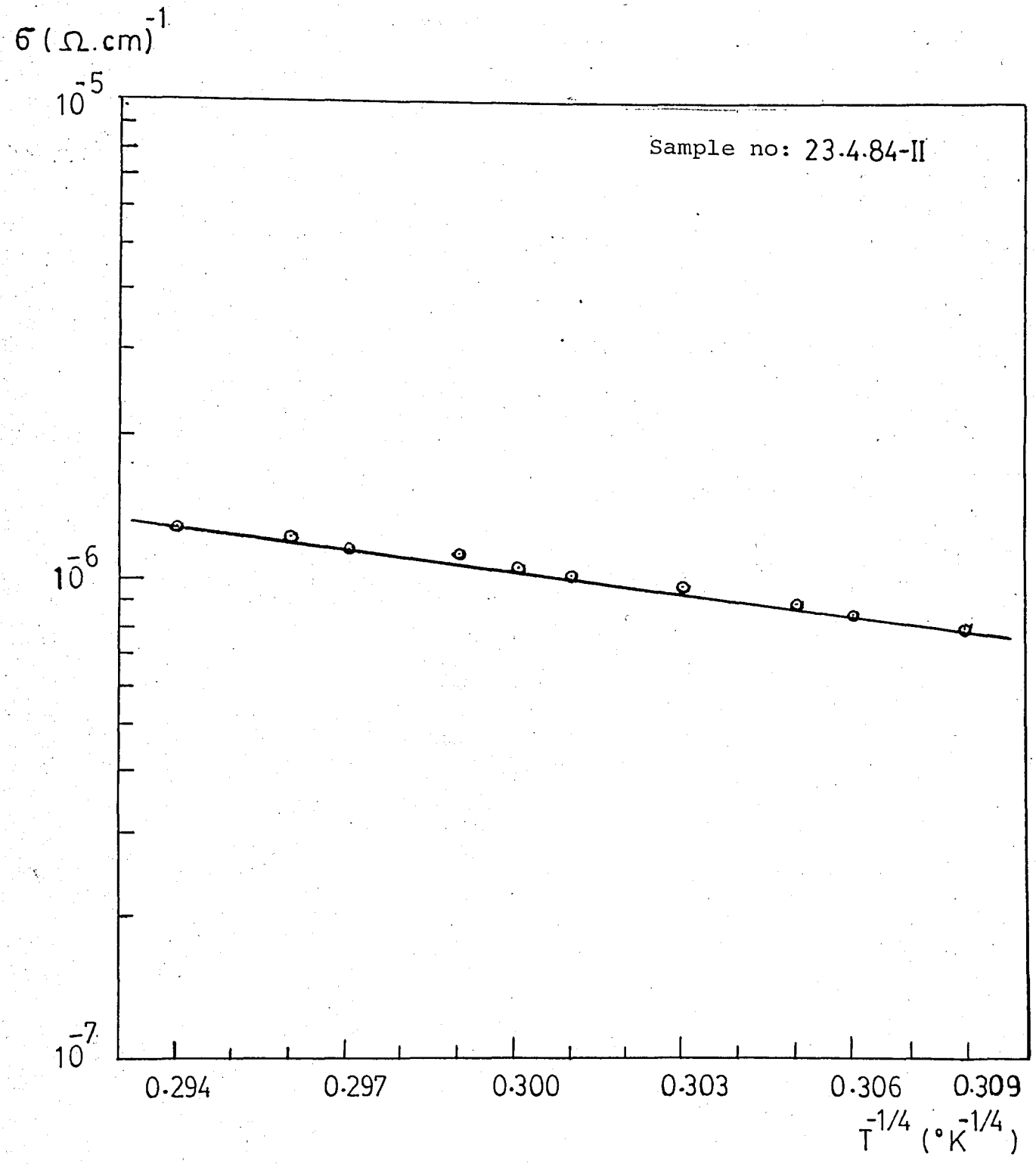

FIGURE 3.12

The variation of Conductivity as a function of $T^{-\frac{1}{4}}$ of the Sample no: 23.4.84-II for the low Temperature Range Between 134°K to 109°K.

IV. CONCLUSIONS

The samples used in this work are prepared by electron beam evaporation under a base pressure of 10^{-7} torr obtained in a conventional vacuum system. The samples consist of an amorphous silicon film of 3000 $\AA$-6000$\AA$ in thickness on which, a layer of aluminum is evaporated as metal electrode.

In order to investigate the electrical properties such as the room temperature conductivity, basic transport mechanisms, the density of states near the Fermi level and the activation energies, d.c measurements are performed in the temperature range from 110°K to 430°K. The I-V measurements at room temperature show that the contacts between the silicon film and the aluminum electrodes are ohmic up to an electric field of 10^3 V/cm. The ohmic behaviour disappears after this region and the current increases exponentially at higher electric fields. At higher electric fields I-V curve obeys the Poole-Frenkel law. The d.c conductivities of the films are around 10^{-5}-10^{-7} $(\Omega\text{-cm})^{-1}$

In the higher temperature range, above 400°K, the conductivity mechanism involved is band-to-band conduction. The activation energies obtained from the slope of $\ln\sigma$-T^{-1} graphs above 400°K are around 0.54-0.8 eV. These activation energies give a mobility gap of 1.1-1.6 eV.

In the high temperature range between 400°K to 285°K the dominant conduction mechanism is different. In this temperature range electrons jump to the tail states closer to the conduction band.

At temperatures between 285°K to 200°K the conductivity mechanism involved is hopping conduction between the nearest neighbours around the Fermi level.

In the low temperature range, below 200°K, and at small electric fields, between 10^2 and 10^3 V/cm. the conductivity of these films obey the $T^{-\frac{1}{4}}$ law as proposed by Mott. These low temperature results are then used to calculate the density of states around the Fermi energy level which is of the order of 10^{20} - 10^{21} $(cm^3\text{-}eV)^{-1}$. The results show that the density of dangling bonds in these films is similar to those prepared by sputtering but is much higher than those prepared by glow-discharge decomposition of silane(SiH_4).

The effects of ageing, annealing and deposition rate during evaporation are also studied. It is observed that the resistivities of the samples deposited at room temperature increase by a factor of 2 or 3 within the first month of preparation. Annealing the samples also increases their resistivities by a factor of 10. However the most effective preparation parameter, in terms of higher resistivity, is the deposition rate. Decreasing the deposition rate from 1.8 A°/ sec to around 0.25 A°/sec increases the resistivities of the films by a factor of 100.

REFERENCES

[1] S.R. ELLIOT, "Defect States in Amorphous Silicon," Philosophical Magazine B, Vol.38, No.4 pq.325-334, 1978

[2] W.E. SPEAR and P.G.LE COMBER, "Investigation of the localized State Distribution in Amorphous Silicon Films," Journal of Non-crystalline Solids, Vol. 8-10, pq. 727-738,1972

[3] N.F. MOTT and E.A. DAVIS, Electronic Processes in Non-crystalline Materials. Oxford : Clarendon Press, 1979.

[4] MORREL H.COHEN, H. FRITZCHE and S.K. OVSHINSKY, "Simple Band Model for Amorphous Semiconducting Alloys," Physical Review Letters, Vol.22, No.2, pq.1065,1068, 1969.

[5] J. STUKE and W. BRENIG, Amorphous and liquid semiconductors. London:Taylor and Prancis Ltd. 1973.

[6] ÇAĞLAYAN, B., "An Environmental Chamber Enabing Electrical and Electro-Optic Measurements," M.S. Thesis, Boğaziçi Üniversity, 1982

[7] P.GE. LE COMBER, Electronic and Structural Properties of Amorphous Semicon ductors. London : Acedemic Press 1972

[8] T.M. DONOVAN and K. HEINEMANN," High Resolution Electronic Microscope Observation of Voids in Amorphous Ge," Physical Review Letters, Vol.27, No.26, pq 1794-1796,1971.

[9] S.K. WONG, B.Y. TONG and P.K. JOHN," High Stable Photosensitive Evaporated Silicon Films," Apply. Phys. Letter, Vol.30, No.10, 1981.

[10] S.K.DEY and B.Y.TONG," Conduction Processes and Threshold Switching in Amorphous Silicon Films," J.Vac. Sci, Technology, Vol.16, No.2 pq.240-243, 1979.

[11] P. DELLAFERRA, R.LABUSH and H.H. ROSCHER, "An alternative Method of Preparing Hydrogen-Doped Evaporated Amorphous Silicon," Phil. Mag.B, Vol. 43, No.1, pq. 169-172, 1981.

[12] D.K. PAUL and S.S. MITRA, "Evaluation of Mott's Parameter for Hopping Conduction in Amorphous Ge, Si and Se-Si," Phys. Rev. Letters, Vol.31, No.16, pq. 1000-1003, 1973.

[13] E.C. FREEMAN and P.PAUL, "Optical Constants of rf-Sputtered Hydrogenated Amorphous Silicon," Phys. Rev. B, Vol.20, pq.716-728, 1979.